Received: 24 February 2024 | Revised: 23 March 2024 | Accepted: 9 April 2024

DOI: 10.1002/jbio.202400068

RESEARCH ARTICLE

JOURNAL OF BIOPHOTONICS

# Spatial targeted delivery of riboflavin with a controlled corneal iontophoresis delivery system in theranostic-guided UV-A light photo-therapy

**Marco Lombardo**[1,2] | **Sebastiano Serrao**[1,2] | **Giuseppe Massimo Bernava**[3] | **Giuseppe Lombardo**[1,3]

[1]Studio Italiano di Oftalmologia, Rome, Italy

[2]Vision Engineering Italy srl, Rome, Italy

[3]CNR-IPCF, Istituto per i Processi Chimico-Fisici, Messina, Italy

**Correspondence**
Marco Lombardo and Giuseppe Lombardo, Studio Italiano di Oftalmologia, Via Livenza 3, 00198 Rome, Italy.
Email: mlombardo@visioeng.it and giuseppe.lombardo@cnr.it

**Funding information**
Lazio Innova, Grant/Award Number: A0613-2023-077528

## Abstract

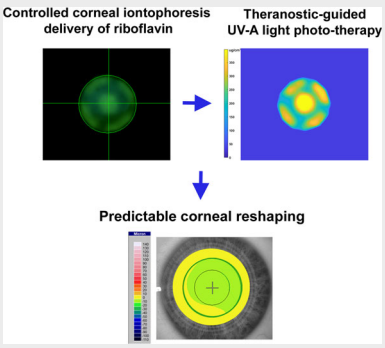


Seven human donor eye globes underwent corneal cross-linking using theranostic UV-A device with accessory corneal iontophoresis system for patterned delivery of a 0.22% riboflavin solution. Theranostic-guided UV-A light illumination assessed riboflavin distribution and treated corneas at 10 mW/cm$^2$ for 9 min with a 5.0-mm beam size. Corneal topography maps were taken at baseline and 2-h post-treatment. Analysis utilized corneal topography elevation data, with results showing controlled riboflavin delivery led to a consistent gradient, with 40% higher levels centrally (248 ± 79 μg/cm$^3$) than peripherally (180 ± 72 μg/cm$^3$ at ±2.5 mm from the center). Theranostic-guided UV-A light irradiation resulted in significant changes in corneal topography, with a decrease in best-fit sphere value (−0.7 ± 0.2 D; $p < 0.001$) and consistent downward shift in corneal elevation map (−11.7 ± 3.7 μm). The coefficient of variation was 2.5%, indicating high procedure performance in achieving significant and reliable corneal flattening.

**KEYWORDS**
corneal cross-linking, corneal iontophoresis, riboflavin, theranostics

## 1 | INTRODUCTION

Corneal cross-linking (CXL) using riboflavin and UV-A light irradiation has been established as a primary treatment option for halting disease progression in individuals affected by keratoconus. Evidences from laboratory data on donor human eyes have demonstrated that the procedure can increase the biomechanical strength of the treated cornea [1, 2].

Clinical studies have observed anterior corneal flattening after CXL treatment of corneal ectasia resulting, in some circumstances, in improved visual acuity, primarily in transepithelial protocols [3, 4]. However, there was considerable variability in the refractive and topographic outcomes of CXL procedures.

Corneal iontophoresis is a method that involves the application of a low electric field to generate an active

**Abbreviation:** CXL, corneal cross-linking.
Marco Lombardo and Giuseppe Lombardo should be considered joint first author.

  

transport of ionized substances into the corneal stroma across the intact epithelium [5]. The ionized substances are driven into the tissue primarily by two mechanisms, such as electromigration (i.e., the motion of molecules based on flow of current) and electro-osmosis (i.e., the motion of the solvent). The passive diffusion of the molecules and the increased tissue permeability induced by electric current may contribute in enhancing the penetration of therapeutic molecules into the stroma, although to a lesser extent than the aforementioned primary mechanisms [6]. The topical iontophoresis strategy has been extensively used for delivering therapeutic molecules into the cornea, including antimicrobials, corticosteroids, and vitamins [7]. Corneal iontophoresis has also been successfully validated for the delivery of riboflavin for treatment of keratoconus with transepithelial CXL, decreasing the overall treatment duration and improving the safety of the procedure [8, 9]. Riboflavin-5-phosphate is a negatively, low molecular weight, charged molecule and therefore an optimal candidate for electrically assisted delivery. Authors have shown in laboratory studies that iontophoresis was able to impregnate the corneal stroma with riboflavin through the intact epithelium and to enhance corneal biomechanical strength [10]. In addition, clinical studies have assessed the long-term safety and efficacy of this approach in the treatment of progressive keratoconus with transepithelial CXL treatment [11–13].

Theranostics is an emergent therapeutic approach in the management of keratoconus by utilizing simultaneous UV-A light mediated fluorescence imaging techniques for assessing riboflavin concentration and enabling targeted photo-activation of the substance in the cornea. The technology has shown to offer a precise and personalized approach for significant improvement of corneal tissue strength, regardless of CXL treatment protocol used, whether it involved removing the corneal epithelium or not [14–16].

By monitoring the concentration and distribution of riboflavin permeating the stroma and its controlled photo-activation under UV-A light in real time, the effectiveness of corneal iontophoresis could be maximized. In this study, we aimed to evaluate a novel corneal iontophoresis device, which is directly controlled by a theranostic UV-A device, for delivering a 0.22% riboflavin ophthalmic solution into the cornea of eye bank donor human eye globes. The iontophoresis device has been designed for patterned delivery of riboflavin through the intact epithelium in order to create a spatial concentration gradient of riboflavin greater in the center of the treated corneal zone compared to the surrounding zones. The amount of riboflavin delivered to the cornea is controlled by modulating the amplitude of the electric current (between 1 and 2 mA), application time (between 4 and 10 min.), and the size and shape of the apertures in contact with the corneal surface. The amplitude of the current determines the rate of flows of electrical charge carriers, which are primarily responsible for the riboflavin delivery. The application time controls the duration of current application and the size and shape of the apertures in contact with the cornea regulate the spatial distribution of riboflavin into the corneal stroma.

The hypothesis of the study was that spatial patterned delivery of riboflavin with higher and consistent levels in the central area of the treated cornea compared to the surrounding areas, followed by theranostic-guided UV-A light irradiation, would lead to a reliable downward shift of corneal shape.

## 2 | EXPERIMENTAL SECTION

Seven human eye globes, not suitable for transplantation, were obtained from the Veneto Eye Bank Foundation (Venezia Zelarino, Italy). The eye globes were explanted between 6 and 12 h after death and immediately preserved at 4°C in corneal storage medium enriched with 15% dextran. All tissues were used for experiments within 48 h. All human eyes were used in compliance with the guidelines of the Declaration of Helsinki for research involving the use of human tissue.

### 2.1 | Theranostic-guided CXL procedure

All eye globes with intact epithelium underwent riboflavin/UV-A CXL procedure using theranostic UV-A device (C4V CHROMO4VIS, Regensight). Description of the UV-A device was given in previous reports [14, 15]. Briefly, the theranostic device integrates a sophisticated system enabling the simultaneous UV-A light-mediated measurement of riboflavin concentration distribution and the photo-activation of the substance within the corneal stroma. In this study, the theranostic device was connected to accessory corneal iontophoresis device (DoRSight, Regensight) for patterned delivery of a 0.22% riboflavin ophthalmic solution (RitSight, Regensight) into the corneal stroma through the intact epithelium. This riboflavin ophthalmic solution has been specifically developed for corneal iontophoresis delivery. The product consists of riboflavin-5-phosphate as primary substance and a double phosphate buffer, which makes the liquid formulation negatively charged to enhance conductivity and facilitate the electromigration of riboflavin into the cornea through the intact epithelium.

The first step of the theranostic-guided CXL treatment consisted in focusing the Placido rings of the medical device's optical head onto the cornea through the

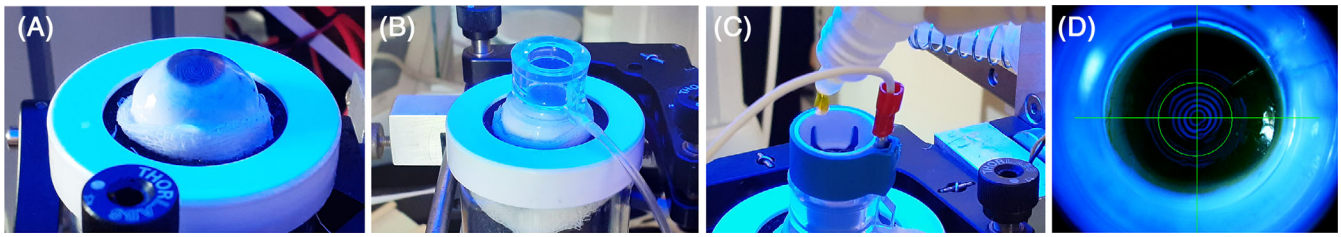


**FIGURE 1** Testing procedure. (A) The donor human eye globe was mounted on a custom-designed eye holder and pre-conditioned. The eye holder could be tilted 90° to perform corneal topography. The corneal iontophoresis delivery system consists of (B) an outer segment, which is suctioned onto the eye and (C) an inner segment, which is filled with riboflavin liquid ophthalmic solution and connected via cable to the theranostic UV-A medical device. (D) At the end of application time, the inner segment is removed, the excess of riboflavin thoroughly dried with a Merocel sponge and the riboflavin corneal concentration distribution measured by theranostic UV-A device.

interaction with an augmented reality system displayed on the touchscreen. Once focusing was completed, an image of the central 5.0 mm of the cornea to treat was acquired by pressing the footswitch to activate a 3 mW/cm$^2$ UV-A light irradiance for 2 s; the measure was recorded as baseline corneal fluorescence signal from the UV-A theranostic device (this signal was subtracted from theranostic measurements obtained after riboflavin application and during UV-A light photo-therapy) [14, 15]. Therefore, the application of the corneal iontophoresis system was done under amber-led light illumination generated by the medical device's optical head to center it onto the pupil of the eye. Application of the active electrode, which is embedded in a plastic bath inner tube, followed by the suctioning of the silicone outer segment to the limbus. The inner tube was placed onto the corneal surface, passing through the outer tube; it was then filled with the riboflavin ophthalmic solution. The passive electrode of the iontophoresis device was connected to a crocodile clip, which was clamped to the optic nerve. Once placed onto the eye, the delivery device was operated through the graphic user interface (GUI) of the theranostic UV-A device; the amplitude of the current generated by the active device ranged between 1.0 and 2.0 mA. In this study, duration of iontophoresis delivery was 7 min in all cases. At the end of riboflavin application, the theranostic UV-A device recorded the fluorescence image of the cornea to estimate the riboflavin corneal concentration [14, 15]. The theranostic measurement was performed over 5.0 mm area by irradiating the cornea under treatment with 3 mW/cm$^2$ UV-A power density for 2 s (as for the baseline measure); the theranostic device processed corneal fluorescence images and provided the operator with a measure estimating the riboflavin spatial concentration distribution in the corneal stroma. The key operational steps of the novel corneal iontophoresis device are summarized in Figure 1. The distal end of the inner tube was designed with apertures of various sizes and shapes in order to enhance the penetration of riboflavin into the central targeted volume of the cornea rather than surrounding tissue volumes. The application time and the sizes and shapes of distal apertures were determined experimentally to reach a targeted spatial concentration distribution of riboflavin in the corneal stroma (data not published). At the end of application time, the delivery device was removed from the eye globe and the cornea underwent 10 mW/cm$^2$ UV-A irradiance for 9 min (5.4 J/cm$^2$ UV-A light energy dose) with a 5.0-mm beam size (Figure 2). At pre-set time intervals during irradiation, the theranostic UV-A device measured the amount of corneal riboflavin photo-activated over the 5.0 mm zone by irradiating the cornea under treatment with 3 mW/cm$^2$ UV-A power density for 2 s (as for the baseline measure). No riboflavin drop was instilled over the corneal surface during UV-A light irradiation in any sample.

## 2.2 | Testing procedure

Each eye globe was kept in a 15% dextran-enriched storage solution at room temperature for 30 minutes before commencing the experiment. The eye globe was then gently mounted into a specially designed holder, with known vertical/horizontal orientation, to guarantee proper centration during the topography measurements. The intraocular pressure (IOP) of the eye globe was adjusted to 18 mmHg by means of a water column, which was connected via a needle to the optic nerve and filled with sterile water for injection. Before the experiment, the pressure of each eye globe was kept constant at 18 mmHg for 20 min in order to achieve a unique *pre-stressing* reference state of the corneal tissue before testing [17–19]. The pressure of the eye was then kept constant at 18 mmHg for the entire duration of the experiment. A commercial air conditioner heat pump was used to maintain the room temperature and humidity constant during the experiment.

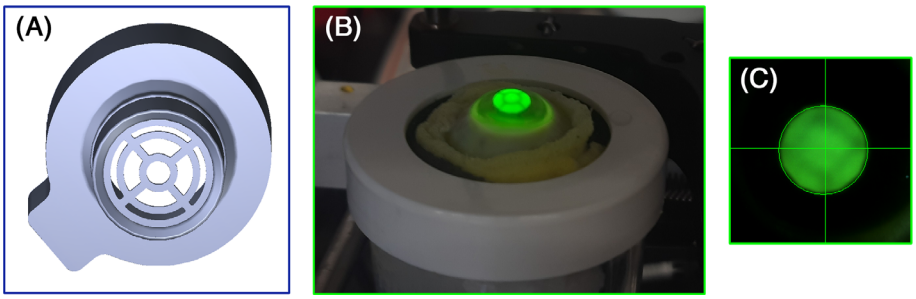


**FIGURE 2** (A) The distal end of the corneal iontophoresis inner segment, which is applied onto the corneal surface, consists of apertures of varying size and shape covering a 10-mm diameter. (B and C) The system allows, under controlled low-current field generated by the theranostic UV-A device, for precise, spatial patterned delivery of riboflavin with higher levels in the central zone than surrounding zones of the treated cornea. This study focused on treating the pre-pupillary central 5.0 mm diameter of the cornea.

Central corneal thickness (CCT) was acquired by Anterior-Segment OCT imaging (AS-OCT; HS-100, Canon) and corneal topography was performed using a Placido disc topographer (Keratron Scout, Optikon 2000). AS-OCT and corneal topography maps were taken at baseline (after the *pre-stressing* procedure) and 2 h after treatment. The elevation maps were evaluated by using internal software of the topographer. Elevation data were expressed using the best-fit sphere (BFS) in diopters (D); the BFS corresponds to the virtual spherocylindric surface that best fits the axial map over central 3.0 mm [20]. In Keratron topographer, the BFS corresponds to the average of the simulated keratometry values, $SimK_{steep}$ and $SimK_{flat}$, which are the average dioptric values of the 3.0 mm central rings of the major and minor axes, respectively. The system calculates the relative elevation based on the deviation of axial map from the BFS; subtraction elevation maps using BFS have been found to be accurate for describing subtle variations in surface geometry and valuable when the true topography must be known [21]. In this study, height difference maps were generated between the elevation data recorded at baseline and 2 h after treatment, after matching the maps at three reference points at 7.0 mm (i.e., outside the treatment zone) from the vertex point ($x = 0$; $y = 0$; corresponding to the highest point in corneal elevation) in order to cancel the tilt; the difference value at the vertex point of the keratograph (expressed in micrometers; μm) was used for analysis.

## 2.3 | Statistical analysis

Data were expressed as mean ± standard deviation with 95% confidence intervals. Sample size was calculated to obtain a mean difference of 10 μm (SD 30%) between the vertex point in subtraction elevation topography maps (i.e., treatment map minus baseline map). A minimum sample size of 5 eye globes was needed to achieve 95% statistical power (ß) at a statistical significance of 5% (α). The targeted mean difference of 10 μm in height difference maps was determined according to the notion that standard CXL treatment achieves on average −1.0 ± 0.8 D corneal apex flattening at 12 months postoperatively [22, 23], theoretically corresponding to a downward shift in anterior corneal elevation of 8 μm with a treatment zone of 5.0 mm [24, 25].

Baseline and postoperative BFS data were compared using paired *t* test. The coefficient of variation (CoV) was calculated to estimate the reliability of the procedure. A regression curve was developed to correlate the downward shift in corneal elevation ($Y$) as a function of the riboflavin spatial concentration ratio ($C_{ratio}$) and the concentration of the substance at ±2.50 mm ($C_{2.5mm}$) as predictors:

$$Y = b_0 + b_1{}^{*}C_{ratio} + b_2{}^{*}C_{2.5mm}, \quad (1)$$

where $b_0$, $b_1$, and $b_2$ are the coefficients of regression and $C_{ratio}$ is the ratio of the riboflavin concentration in the center of treated cornea with respect to the mean concentration of the substance at ±2.5 mm from the center.

## 3 | RESULTS AND DISCUSSION

All samples underwent through testing and the process was successfully completed in all cases. The mean donor age was 70 ± 7 years. The mean cadaver time was 12 ± 4 h. At baseline, the mean CCT was 581 ± 56 μm; it did not change at the end of experiments (593 ± 63 μm). During the experiments, the room temperature was 25.6 ± 0.8°C and the relative humidity was 54 ± 3%. Testing on eye bank donor eye globes was performed under monitoring of IOP and environmental parameters to assess the effectiveness of the new strategy for spatial targeted

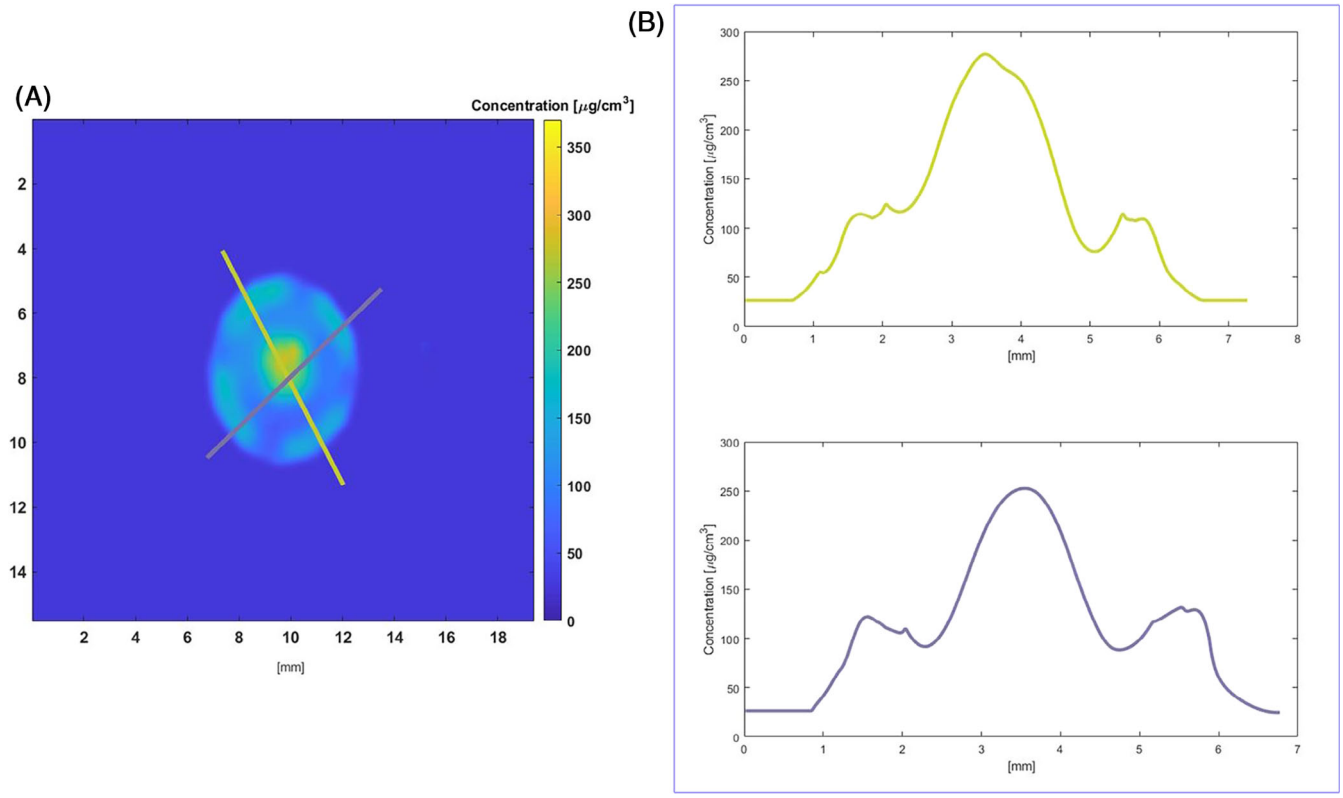


**FIGURE 3** Delivery of riboflavin into the cornea through the corneal iontophoresis-controlled system allows for achieving targeted concentration distribution of the substance into the cornea with averagely 40% higher levels in the central zone of the treated cornea compared to surrounding areas (±2.5 mm from center). In (A and B), the real-time theranostic UV-A device monitoring system of corneal riboflavin concentration distribution (the bar indicates concentration in μg/cm$^3$) and the resulting concentration profiles along two axes, respectively.

delivery of riboflavin into the cornea prior to UV-A light irradiation in theranostic-guided CXL procedure. Several factors make the use of the whole eye preferable for preclinical testing of new medical devices: temperature and humidity of the environment, which may influence corneal biomechanics, can be monitored; the corneal tissue can be mounted with respect to its correct vertical/horizontal orientation and native boundary conditions of the cornea are preserved (the procedure is minimally invasive for the corneal tissue); the applied stress is generated by monitored IOP and a unique *pre-stressing* reference state can be achieved for all samples. The use of corneal topography allows detailed characterization of the corneal surface with micrometric resolution and data can be easily analyzed using standardized units of measure, which are relevant in the clinical setting and facilitate the translation of findings into practical applications.

After 7 min of corneal iontophoresis application, the average peak corneal riboflavin concentration was 248 ± 79 μg/cm$^3$; a pseudo-Gaussian distribution concentration profile was found in all samples, with a mean corneal riboflavin concentration of 180 ± 72 μg/cm$^3$ at ±2.50 mm from the central concentration peak (Figure 3). The ratio of riboflavin concentration between the center and ±2.50 mm surrounding zones was 1.4 ± 0.2. At the end of UV-A light irradiation, the average corneal riboflavin concentration decreased by 57 ± 7% (resulting 109 ± 43 μg/cm$^3$) at the center and by 54 ± 6% (resulting 83 ± 34 μg/cm$^3$) at ±2.50 mm surrounding zone. The average BFS significantly flattened from 43.1 ± 1.2 D to 42.4 ± 1.3 D after treatment ($p < 0.001$). The induced change at the vertex point of subtraction elevation topography maps was −11.7 ± 3.7 μm (95% confidence interval [CI]: −10.3 to −13.1 μm; CoV: −0.3 μm); the CoV was 2.5% of the average downward shift, thus confirming the high performance of the procedure in achieving a repeatable effect on corneal shape change. A representative case is shown in Figure 4. A statistically significant correlation was found between the level of downward shift in corneal elevation and the predictors, including the ratio of riboflavin concentration and the concentration at ±2.50 mm ($R = 0.92$; $p = 0.02$; Figure 5). The outcome data of the laboratory study were summarized in Table 1.

The concentration of riboflavin plays a crucial role in generating covalent chemical bonds between stromal

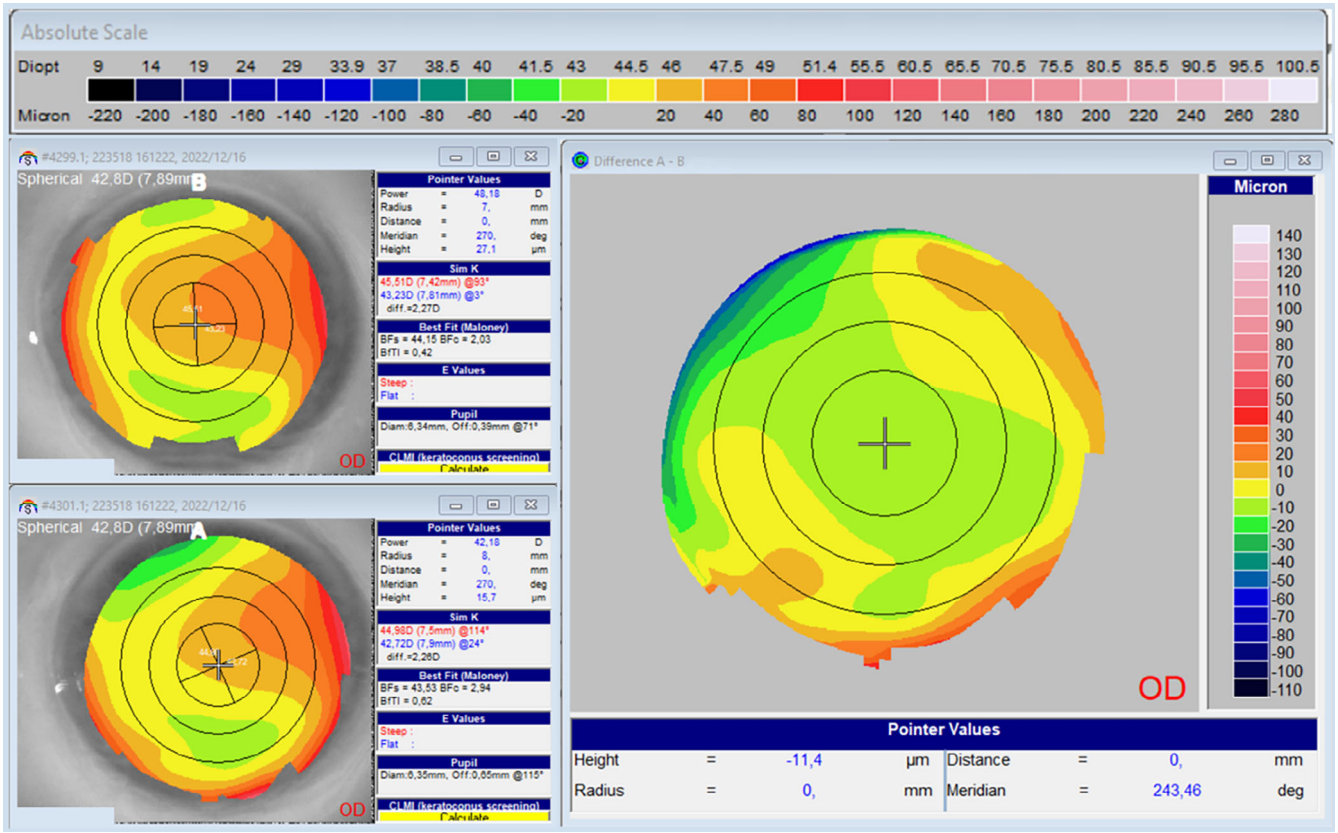


**FIGURE 4** The subtraction elevation topography map for sample code 223518 (see Table 1) demonstrated a significant −11.4 µm downward shift following theranostic-guided CXL treatment with spatial targeted delivery of 0.22% riboflavin and 5.0 mm UV-A light beam irradiation. This finding evidenced a measurable change in the anterior corneal topography of the sample after treatment. CXL, corneal cross-linking.

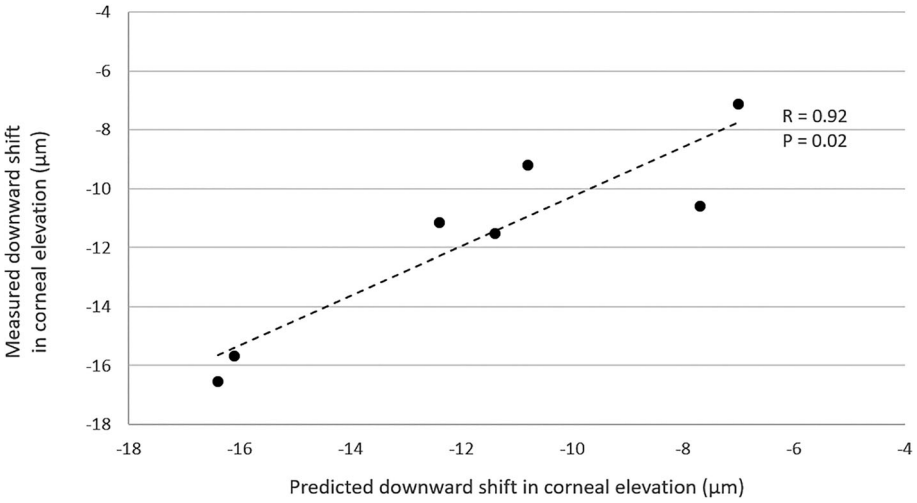


**FIGURE 5** Correlation between the downward shift in corneal elevation at vertex point induced by theranostic-guided CXL treatment with corneal iontophoresis-controlled system and the outcome predicted by a two-predictor model incorporating the spatial concentration distribution of riboflavin ($C_{ratio}$) and the concentration of the substance at ±2.5 mm with respect to peak concentration ($C_{2.5mm}$). Each symbol represents an eye bank human donor eye ($n = 7$). CXL, corneal cross-linking.

proteins in the cornea [26–28]. An improved understanding of CXL procedure has led to the theorization that the treatment could also be used to produce a predictable and reproducible corneal shape change. In this study, controlled delivery of riboflavin and UV-A light irradiation were centered onto the pupil in order to test the effect of theranostic-guided UV-A light photo-therapy on central corneal flattening; the UV-A device, however, allows for focusing on the specific area of interest, such as the keratoconus apex, using the integrated blue light Placido disc system and the amber lights illumination system.

**TABLE 1** Main laboratory findings.

| Sample code | Peak riboflavin concentration (μg/cm$^3$) | ±2.5 mm zone riboflavin concentration (μg/cm$^3$) | Corneal BFS[a] at baseline (D) | Corneal BFS[a] after treatment (D) | Downward shift at vertex point of corneal height difference maps (μm) |
|---|---|---|---|---|---|
| Code 223464 | 180 | 130 | 43.34 | 42.67 | −7.7 |
| Code 223518 | 280 | 190 | 44.15 | 43.53 | −11.4 |
| Code 224482 | 267 | 180 | 42.74 | 42.11 | −12.4 |
| Code 222412 | 256 | 141 | 43.99 | 43.60 | −7.0 |
| Code 230984 | 110 | 80 | 41.30 | 40.64 | −10.8 |
| Code 231007 | 295 | 250 | 41.72 | 40.57 | −16.1 |
| Code 232077 | 350 | 290 | 44.15 | 43.54 | −16.4 |
| M ± SD | 248 ± 79 | 180 ± 72 | 43.06 ± 1.18 | 42.38 ± 1.33 | −11.7 ± 3.7 |

*Note*: In the bottom row, data are expressed as mean (M) ± standard deviation (SD).
[a]BFS: best-fit sphere.

This ensures that the treatment is accurately directed toward the desired corneal region to flatten.

The authors have predicted that under appropriate photo-activation by UV-A light, the tissue biomechanical response could be selectively differentiated according to the controlled spatial distribution of riboflavin concentration and may cause the cornea to deform to a defined shape [29–31]. Based upon these considerations, controlling the riboflavin spatial concentration distribution in the corneal stroma, the UV-A light intensity and/or treatment time would result in different amount and spatial distribution of induced cross-linking bonds among stromal proteins and therefore in a different increase in corneal stiffness. In this study, the application time of riboflavin (7 min) and the UV-A light irradiation protocol (10 mW/cm$^2$ for 9 min with 5.0 mm beam size) were the same for all eyes; this approach helped ensure that the primary hypothesis of the study was accurately tested and any observed effects could be attributed directly to non-uniform spatial concentration distribution of stromal riboflavin prior to UV-A light illumination. On the other hand, manual application of riboflavin onto the cornea, which likely generates uniform concentration distribution across the stroma [32], combined with a gradient change of energy dose during UV-A illumination did not lead to effective corneal flattening, as theorized by Roy et al. [33] In a pilot study on 50 patients with keratoconus, Shetty et al. [34] compared the effect on corneal tomography of four different UV-A light irradiation protocols after the application of 0.1% riboflavin ophthalmic solution for 20 min on de-epithelialized corneas. The authors found that a 9.0 mm beam diameter UV-A light illumination with a gradient change of energy dose in three to five circles (with higher energy in the central than peripheral circles, ranging from 15 to 0.5 J/cm$^2$) centred on the steepest curvature provided lower decrease in maximum keratometry value ($K_{max}$) compared with a uniform UV-A light illumination treatment. Previous reports have shown that higher UV-A light power densities and energy dose were associated with a structural weakening of the corneal tissue [35, 36]. Due to the lack of experimental studies supporting the efficacy of a gradient distribution of UV-A light fluence in achieving a predictable flattening the cornea, it is difficult to draw significant conclusions on the hypothesis and methodology proposed by these authors [33, 34]. The absence of real-time monitoring of corneal riboflavin concentration data also makes it challenging to determine the primary cause of their unsuccessful outcomes [14, 15, 30–32].

The theory supporting the hypothesis that non-homogeneous photopolymerization of the corneal tissue may cause a more pronounced flattening of the anterior cornea than homogeneous photopolymerization was based on the characteristics of stromal architecture [37]. The microstructural organization of the human cornea has been deeply investigated by many authors who reported regional differences in the histology and biomechanics of the corneal tissue [38–41]. Differences in the regional response of the cornea in relation to the photopolymerization profile may depend on the different postoperative strength distribution in the specialized architecture of stromal collagen lamellae induced by theranostic-mediated UV-A light photo-activation [42–45].

Further research will include analysis of whether the amount of the downward shift in anterior corneal elevation induced by theranostic UV-A photo-therapy using controlled corneal iontophoresis may be influenced by the application time of riboflavin and/or by the UV-A light beam width [8]. In this system, the delivery time of corneal iontophoresis can be set from

4 to 10 min and the UV-A light beam from 5.0 to 9.0 mm diameter.

A corneal riboflavin concentration ≥140 μg/cm$^3$ has been shown to be sufficient for inducing significant mechanical stiffening of the corneal stroma when delivering 5.4 J/cm$^2$ UV-A energy dose [46]. In the previous report [10], the authors demonstrated that transepithelial CXL treatment using corneal iontophoresis was effective in improving tissue stiffness in inflation experiments of human donor eye globes. The same authors [16], using theranostic UV-A device, have measured in human donor eye globes a mean riboflavin corneal concentration of 176 ± 8 μg/cm$^3$ (30% lower than found in the present study) using iontophoresis-assisted uniform delivery of 0.1% riboflavin ophthalmic solution at 1 mA current for 5 min.

## 4 | CONCLUSION

In this study, a corneal iontophoresis-controlled system designed for spatial targeted delivery of riboflavin during theranostic-guided UV-A light photo-therapy was tested. Impregnation of the cornea with a consistent spatial concentration gradient of riboflavin led to an efficient and precise shape change of the cornea under theranostic UV-A light-mediated illumination. These findings supported the hypothesis that riboflavin spatial concentration distribution may play a crucial role in the photopolymerization process of the cornea and provided further insight into potential application for theranostic-guided UV-A light photo-therapy in corneal reshaping procedures. Clinical research is necessary to explore this possibility and determine the effectiveness of this novel procedure in achieving a targeted corneal flattening in individuals.

### AUTHOR CONTRIBUTIONS

Giuseppe Lombardo and Marco Lombardo were involved in conceptualization, investigation, writing–original draft, and project management. Sebastiano Serrao and Giuseppe Massimo Bernava were involved in the investigation, data analysis, review, and editing original draft.

### ACKNOWLEDGMENTS

This study was in part funded by Lazio Innova in the framework of FESR 2021–2027 program with grant number A0613-2023-077528.

### CONFLICT OF INTEREST STATEMENT

Sebastiano Serrao declares no financial or commercial conflict of interest. Giuseppe Massimo Bernava declares no financial or commercial conflict of interest. Marco Lombardo is co-inventor on issued patents (IT102016000007349; 102019000010341; WO2017130043A1) related to this work. Giuseppe Lombardo is co-inventor on issued patents (IT102016000007349; 102019000010341; WO2017130043A1) related to this work.

### DATA AVAILABILITY STATEMENT

Research data are not shared.

### ORCID

*Marco Lombardo* https://orcid.org/0000-0001-8842-7102
*Sebastiano Serrao* https://orcid.org/0000-0002-4141-6462
*Giuseppe Massimo Bernava* https://orcid.org/0000-0001-8024-1338
*Giuseppe Lombardo* https://orcid.org/0000-0002-9416-967X

### REFERENCES

[1] E. Spoerl, M. Huhle, T. Seiler, *Exp. Eye Res.* **1998**, *66*, 97.
[2] I. M. Beshtawi, C. O'Donnell, H. Radhakrishnan, *J. Cataract. Refract. Surg.* **2013**, *39*, 451.
[3] S. M. Ng, M. Ren, K. B. Lindsley, B. S. Hawkins, I. C. Kuo, *Cochrane Database Syst. Rev.* **2021**, *3*, CD013512.
[4] S. Nath, C. Shen, A. Koziarz, L. Banfield, B. Nowrouzi-Kia, M. A. Fava, W. G. Hodge, *Ophthalmology* **2021**, *128*, 1150.
[5] T. Gratieri, V. Santer, Y. N. Kalia, *Exp. Opin. Drug Deliv.* **2017**, *14*, 1091.
[6] N. Abla, A. Naik, R. H. Guy, Y. N. Kalia, *J. Controlled Release* **2005**, *108*, 319.
[7] E. Eljarrat-Binstock, A. J. Domb, *J. Controlled Release* **2006**, *110*, 479.
[8] A. Arboleda, L. Kowalczuk, M. Savoldelli, C. Klein, S. Ladraa, M. C. Naud, M. C. Aguilar, J. M. Parel, F. Behar-Cohen, *Invest. Ophthalmol. Vis. Sci.* **2014**, *55*, 2731.
[9] M. Lombardo, D. Giannini, G. Lombardo, S. Serrao, *Ophthalmology* **2017**, *124*, 804.
[10] M. Lombardo, S. Serrao, M. Rosati, P. Ducoli, G. Lombardo, *J. Cataract. Refract. Surg.* **2014**, *40*, 1706.
[11] M. Lombardo, S. Serrao, G. Lombardo, D. Schiano-Lomoriello, *J. Cataract. Refract. Surg.* **2019**, *45*, 992.
[12] G. Bikbova, M. Bikbov, *Acta Ophthalmol.* **2016**, *94*, e600.
[13] A. M. Roszkowska, G. W. Oliverio, K. Hydzik-Sajak, M. De Crescenzo, P. Aragona, *Int. Ophthalmol.* **2023**, *43*, 3601.
[14] G. Lombardo, G. M. Bernava, S. Serrao, A. M. Roszkowska, M. Lombardo, *J. Cataract. Refract. Surg.* **2023**, *49*, 635.
[15] G. Lombardo, G. M. Bernava, S. Serrao, M. Lombardo, *J. Biophotonics* **2022**, *15*, e202200218.
[16] G. Lombardo, S. Serrao, M. Lombardo, *Graefes Arch. Clin. Exp. Ophthalmol.* **2020**, *258*, 829.
[17] B. L. Boyce, R. E. Jones, T. D. Nguyen, J. M. Grazier, *J. Biomech.* **2007**, *40*, 2367.
[18] B. L. Boyce, J. M. Grazier, R. E. Jones, T. D. Nguyen, *Biomaterials* **2008**, *29*, 3896.
[19] H. Hennighausen, S. T. Feldma, J. F. Bille, A. D. McCulloch, *Invest. Ophthalmol. Vis. Sci.* **1998**, *39*, 253.
[20] R. K. Maloney, S. J. Bogan, G. O. Waring, *Am. J. Ophthalmol.* **1993**, *115*, 31.

[21] T. O. Salmon, D. G. Horner, *Optom. Vis. Sci.* **1995**, *72*, 800.
[22] J. Li, P. Ji, X. Lin, *PLoS One* **2015**, *10*, e0127079.
[23] S. Serrao, G. Lombardo, M. Lombardo, *Int. Ophthalmol.* **2022**, *42*, 337.
[24] C. R. Munnerlyn, S. J. Koons, J. Marshall, *J. Cataract. Refract. Surg.* **1998**, *14*, 46.
[25] F. Manns, A. Ho, J.-M. Parel, W. Culbertson, *J. Cataract. Refract. Surg.* **2002**, *28*, 766.
[26] P. Kamaev, M. D. Friedman, E. Sherr, D. Muller, *Invest. Ophthalmol. Vis. Sci.* **2012**, *53*, 2360.
[27] J.-T. Lin, *J. Ophthalmol. Vis. Neurosci.* **2018**, *3*, 1.
[28] J. T. Lin, *Invest. Ophthalmol. Vis. Sci.* **2018**, *59*, 431.
[29] J.-T. Lin, D.-C. Cheng, *PLoS One* **2017**, *12*, e0175002.
[30] R. Schumacher, M. Mrochen, J. Wernli, M. Bueeler, T. Seiler, *Invest. Ophthalmol. Vis. Sci.* **2012**, *53*, 762.
[31] A. Semchisten, M. Mrochen, V. Semchisten, *Photochem. Photobiol.* **2015**, *91*, 1403.
[32] M. Lombardo, N. Micali, V. Villari, S. Serrao, *Invest. Opthalmol. Vis. Sci.* **2016**, *57*, 476.
[33] A. S. Roy, W. J. Dupps Jr., *Invest. Ophthalmol. Vis. Sci.* **2011**, *52*, 9174.
[34] R. Shetty, N. Pahuja, T. Roshan, R. Deshmukh, M. Francis, A. Ghosh, A. S. Roy, *J. Refract. Surg.* **2017**, *33*, 676.
[35] J. Wernli, S. Schumacher, E. Spoerl, M. Mrochen, *Invest. Ophthalmol. Vis. Sci.* **2013**, *54*, 1176.
[36] E. Lanchares, M. A. del Buey, J. A. Cristóbal, L. Lavilla, B. Calvo, *Graefes Arch. Clin. Exp. Ophthalmol.* **2011**, *249*, 1223.
[37] A. Daxer, P. Fratzl, *Invest. Ophthalmol. Vis. Sci.* **1997**, *38*, 121.
[38] M. K. Smolek, B. E. McCarey, *Invest. Ophthalmol. Vis. Sci.* **1990**, *31*, 1087.
[39] M. K. Smolek, *Invest. Ophthalmol. Vis. Sci.* **1993**, *34*, 2962.
[40] K. M. Meek, T. Blamires, G. F. Elliot, T. J. Gyi, C. Nave, *Curr. Eye Res.* **1987**, *6*, 841.
[41] Y. Komai, T. Ushiki, *Invest. Ophthalmol. Vis. Sci.* **1991**, *32*, 2244.
[42] D. Park, E. Perez, D. Miller, *Invest. Ophthalmol. Vis. Sci.* **1995**, *36*, 39.
[43] T. J. Shin, R. P. Vito, L. W. Johnson, B. E. McCarey, *J. Biomech.* **1997**, *30*, 497.
[44] J. Ø. Hjortdal, *J. Biomech.* **1996**, *29*, 931.
[45] Z. Han, X. Sui, D. Zhou, C. Zhou, Q. Ren, *J. Refract. Surg.* **2013**, *29*, 282.
[46] G. Lombardo, V. Villari, N. Micali, N. Leone, C. Labate, M. P. De Santo, M. Lombardo, *J. Biophotonics* **2018**, *11*, e201800028.

## AUTHOR BIOGRAPHIES

**Marco Lombardo** graduated in Medicine and Surgery in 1999 (summa cum laude) and specialized in Ophthalmology in 2003 (summa cum laude); he earned his PhD in Biomedical Engineering and Computer Science in 2007. He has developed a number of innovative medical devices and ophthalmic formulations for the prevention and treatment of major eye diseases. He published more than 100 papers in peer-reviewed scientific journals and co-authored six books in the fields of human optics, corneal biomechanics, and corneal surgery. He is a co-inventor of three patents.

**Sebastiano Serrao** graduated with honors in Medicine and Surgery and specialized with honors in Ophthalmology; he holds a PhD in Refractive Surgery. He is expert in the field of anterior segment eye surgery and has strong technical competence in clinical validation of innovative products for eye care. He serves, on a regular basis, as reviewer for more than 10 scientific journals in the field of applied optics, microscopy, and vision science. He published more than 80 articles in peer-reviewed scientific journals and co-authored five books in the field of Ophthalmology.

**Giuseppe Massimo Bernava** holds a BSc in Computer Engineering and PhD in Computer Science. He is research technologist at the Institute for Chemical and Physical Processes of the National Research Council (CNR–IPCF) in Italy. He is expert in application of deep learning in the biomedical field; over the years, he has been involved in the design and development of multi-platform systems for the development of intelligent interfaces primarily to define and customize tele-rehabilitation services. He has published more than 20 papers in peer-reviewed journals.

**Giuseppe Lombardo** is an electronic engineer with PhD in electronics and Master's Degree in biomedical engineering. He is the first researcher at the Institute for Chemical and Physical Processes of the National Research Council (CNR–IPCF) in Italy. His main scientific interests are devoted to study of optical and mechanical properties of soft matter. He is also keen in numerical modeling and has experience in image processing and pattern recognition algorithms application in biomedical images. He has published more than 100 papers in peer-reviewed journals and is co-inventor in seven patents.

**How to cite this article:** M. Lombardo, S. Serrao, G. M. Bernava, G. Lombardo, *J. Biophotonics* **2024**, *17*(7), e202400068. https://doi.org/10.1002/jbio.202400068